Eur. Phys. J. D **34**, 177–182 (2005)
DOI: 10.1140/epjd/e2005-00135-4

THE EUROPEAN PHYSICAL JOURNAL D

Stern-Gerlach studies of organometallic sandwich clusters

K. Miyajima[1], M.B. Knickelbein[2], and A. Nakajima[1,3,a]

[1] Department of Chemistry, Faculty of Science and Technology, Keio University, 3-14-1 Hiyoshi, Kohoku-ku, 223-8522 Yokohama, Japan
[2] Chemistry Division, Argonne National Laboratory, Argonne, 60439 Illinois, USA
[3] CREST, Japan Science and Technology Agency (JST), c/o Department of Chemistry, Keio University, 223-8522 Yokohama, Japan

Received 6 September 2004
Published online 13 July 2005 –

Abstract. Stern-Gerlach type magnetic deflection measurements were performed for two types of multiple sandwich clusters: vanadium-benzene $V_n(C_6H_6)_{n+1}$ and terbium-cyclooctatetraene $Tb_n(C_8H_8)_{n+1}$. Beams of $V_n(C_6H_6)_{n+1}$ clusters ($n = 1-4$) showed symmetric broadening induced by the inhomogeneous field, indicating free spin behavior similar to that displayed by isolated paramagnetic atoms. By contrast, beams of $Tb_n(C_8H_8)_{n+1}$ clusters displayed one-sided deflection, indicating that fast spin relaxation occurs within the clusters. The difference in the magnetic deflection behavior exhibited by these two systems is explained by their electronic structures, specifically the bonding characteristics between metal atoms and ligand molecules.

PACS. 36.40.Cg Electronic and magnetic properties of clusters

1 Introduction

Multi-nuclear organometallic sandwich clusters (or complexes) are novel organometallic species whose one-dimensional structures are determined by metal-ligand interactions confined to a single molecular axis. Thus far, there have been many examples of such complexes generated in vacuo; their geometric and electronic structures have been investigated using a variety of molecular beam-based techniques [1]. Because these complexes contain transition metals or lanthanide metals as constituents, it may be anticipated that they may be paramagnetic or even magnetically ordered. Using molecular beam deflection techniques, the size dependence of bare (unligated) metal clusters' magnetic moments have been measured in a series of studies during the 1990's [2–6]. However for paramagnetic organometallic complexes, there has been only a single report of molecular beam deflection analysis of magnetic properties, by Amirav and Navon [7]. The intrinsic microscopic magnetic properties of magnetic molecules and clusters can be revealed by experiments conducted in the gas phase (i.e., in the absence of a solvent or matrix). The elucidation of the magnetic properties of gas-phase organometallic clusters will thus be an important task underlying the rational design of future novel magnetic materials, for example single molecule magnets.

In this contribution, we present the results of Stern-Gerlach molecular beam deflection studies of two different types of organometallic multi-decker sandwich clusters: vanadium-benzene $V_n(C_6H_6)_{n+1}$ and terbium-cyclooctatetraene $Tb_n(C_8H_8)_{n+1}$. These systems were chosen as prototypes for sandwich complexes containing transition metals (M) and lanthanide (Ln) metals, respectively. The $V_n(C_6H_6)_{n+1}$ clusters are characterized by covalent bonding between vanadium 3d orbitals and benzene LUMOs [8,9]. Their unique electronic structure has been probed by photoionization efficiency measurements [8]. On the other hand, bonding in $Ln_n(C_8H_8)_{n+1}$ sandwich clusters has been found to be highly ionic in nature [10–12] as a result of charge-transfer from Ln metal atoms to C_8H_8 ligands. Although the multidecker sandwich clusters have been anticipated to be highly anisotropic molecular magnets, their magnetic properties have remained uncharacterized experimentally. For vanadium-benzene clusters, the existence of unpaired electrons on the V atoms have been predicted rise to give to their paramagnetism [9]. By contrast, for Ln-C_8H_8 clusters, unpaired $4f$ electrons within the Ln ions determine the magnetic properties. Since $4f$ electrons are effectively shielded from interaction with external ligand fields by the outer-lying $5s^2$ and $5p^6$ electrons, magnetic properties of Ln containing clusters are essentially ascribed to those of Ln free ions, Ln^{2+} and Ln^{3+}. Therefore the size as determined by the number of layers in a multi-decker sandwich cluster may account for the overall magnetic moments. To our knowledge, there have been no measurements of incremental magnetic moment for multi-decker sandwich complexes. There are a

[a] e-mail: nakajima@chem.keio.ac.jp

few reports on the magnetic susceptibilities of the ionic sandwich lanthanide complexes: $K^+[Ln(C_8H_8)_2]^-$ and $Ln(C_8H_8)_2Cl{\cdot}2THF$ [13]. These Ln complexes (Ln = Ce, Pr, Nd, Sm and Tb), are all paramagnetic. In the present work, we discuss the magnetic properties of organometallic sandwich clusters as determined in the gas phase by the Stern-Gerlach deflection method.

2 Experimental section

In the present study, terbium was selected from among the various lanthanide metals due to its large magnetic moment. Vanadium was selected from among the transition metals because an unpaired electron is left on each V atom in a nonbonding d orbital. The magnetic moments of $V_n(C_6H_6)_{n+1}$ and $Tb_n(C_8H_8)_{n+1}$ complexes were measured by molecular beam magnetic deflection — a variation on the classic Stern-Gerlach experiment used originally to determine the magnetic moments of atoms. In this approach, species that can be produced only in small amounts and/or that are highly reactive can be studied without the perturbing influences of solvents, matrices or self-reaction/polymerization. Furthermore, the use of a position-sensitive time-of-flight mass spectrometer for detection enables us to obtain deflection information for clusters with various compositions and sizes (n, m) simultaneously. The experiments and analysis procedures have been described in detail elsewhere [14]. Briefly, metal atoms were produced by focusing the second harmonic output of Nd^{3+}:YAG laser (∼30 mJ/pulse, 25 Hz) onto a target rod within a fast flow cluster source. The atomic vapor was carried by a continuous stream of helium into a flow tube reactor, where ligand vapor (C_6H_6 or C_8H_8) was injected. The subsequent reaction of the metal atoms and benzene form a variety of product species, the dominant fraction of which consists of the full sandwich complexes, $M_n(C_6H_6)_{n+1}$ or $Ln_n(C_8H_8)_{n+1}$. The mixture of helium and organometallic complexes expanded into vacuum through a 1.5 mm diameter nozzle at the end of the flow tube. The resulting supersonic free jet was collimated into a molecular beam using a series of skimmers and orifices. The collimated molecular beam passed into a high vacuum chamber, where it passed through the gap of a dipole gradient electromagnet capable of producing an inhomogeneous magnetic field, with gradients $\partial B/\partial z$ up to ∼210 T/m and B fields up to ∼1.2 T. The complexes were detected 0.9 m downstream of the deflection magnet using laser photoionization time-of-flight (TOF) mass spectrometry employing an ArF excimer laser as the photoionization source. The TOF spectrometer was operated in the position-sensitive mode [15], which maps the spatial distribution of the molecular beam along the z-axis (parallel with the magnetic field) onto the time domain. Between 800−2000 spectra were averaged in a digital oscilloscope with the magnetic field on, and then again with the field off. The deflection of the molecular beam was determined by quantitatively comparing the temporal profiles of the mass peaks in the field-on TOF spectrum with those of the field-off spectrum. The relation between the deflection magnitude and a gradient field has been calibrated by studying the Ho atom ($^6H_{15/2}$).

In Stern-Gerlach studies of atoms and clusters such as those reported here, the z-component of magnetic moment μ_z of the species under investigation is given by

$$\mu_z = \frac{f}{t_{\rm arr}} \frac{mV^2}{LD\,\mu_{\rm B}} \frac{\Delta t}{(\frac{\partial B}{\partial z})}, \tag{1}$$

where the factor f is an instrumental constant, $t_{\rm arr}$ is the arrival time of the target cluster, m is mass of the cluster, V is a cluster beam speed, D and L are the length of the magnet and the distance from the final collimating slit to the detector, Δt is the time difference from the TOF peak center of the cluster, and $(\partial B/\partial z)$ is magnetic gradient, respectively.

The average position of deflected profile (computed as the peak first moment), is the quantity measured in determining net beam deflections. The beam shifts are determined as the difference in first moments between the zero-field beam profile and the profile recorded with the field applied. For superparamagnetic clusters (i.e., those in which intramolecular spin relaxation occurs on a timescale faster than the flight time through the magnetic field) the peak shift can be described by the Langevin model [16], and it can be approximated by the Curie law under the condition of $\mu B \ll kT$

$$\langle M_z \rangle = \frac{\mu^2 B}{3\,kT}. \tag{2}$$

Here the time averaged effective magnetic moment $\langle M_z \rangle$ is related to the true cluster moment μ. Thus the magnetic moment μ (in $\mu_{\rm B}$ units) can be obtained from the deformation of (1),

$$\mu = \frac{1}{\mu_{\rm B}} \sqrt{\frac{f}{t_{\rm arr}} \frac{mV^2}{LD}\, 3\,kT\, \frac{\Delta t_{\rm delay}}{B\frac{\partial B}{\partial z}}} \tag{3}$$

where $\Delta t_{\rm delay}$ is the shift of the peak, B is the magnetic field in T. The last term indicates that $\Delta t_{\rm delay}$ should be in proportional to $B(\partial B/\partial z)$ in this model. Since the magnitude of B is roughly proportional to that of $(\partial B/\partial z)$ in the case of this set-up, the $(\partial B/\partial z)$ dependence of the peak delay $\Delta t_{\rm delay}$ is quadratic.

3 Results and discussion

3.1 $V_n(C_6H_6)_{n+1}$ clusters

Figure 1 shows photoionization mass spectra of vanadium-benzene clusters generated at source temperatures of 151 and 63 K. Labeled peaks corresponding to "complete" sandwich $V_n(C_6H_6)_{n+1} = (n, n+1)$ complexes appear prominently. Small quantities of incomplete sandwich clusters (e.g. "half" sandwich clusters containing an uncapped metal atom, or clusters which contain excess benzene molecules) are also produced. Under colder source

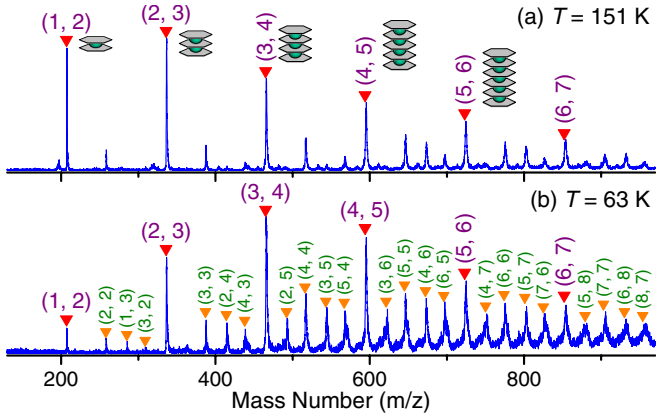

Fig. 1. Mass spectra of vanadium-benzene clusters: $V_n(C_6H_6)_{n+1}$ at (a) $T = 151$ and (b) 63 K.

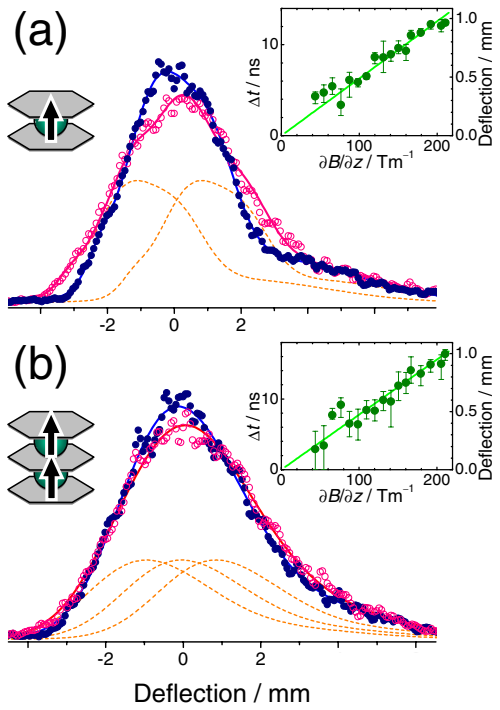

Fig. 2. Broadening of TOF peak of (a) $V(C_6H_6)_2$ and (b) $V_2(C_6H_6)_3$ by the magnetic field gradient ($T = 154$ K, $\partial B/\partial z = 192$ Tm^{-1}). The dotted lines indicate the beamlets which have the same shape of undeflected peak. The separation between adjacent beamlets, Δt, was obtained from curve fitting.

conditions ($T = 63$ K), larger incomplete sandwich clusters such as (n, n), $(n, n+2)$, and $(n, n+3)$ become prominent, as shown in Figure 1b.

Figure 2 shows a detailed view of the position sensitive time-of-flight (PS-TOF) mass peaks corresponding to $V(C_6H_6)_2$ and $V_2(C_6H_6)_3$ recorded with and without the magnetic field applied. The effect of the inhomogeneous magnetic field is to symmetrically broaden the spatial distribution of the $V_n(C_6H_6)_{n+1}$ complexes in the $\pm z$-direction. This behavior is qualitatively the same as would be observed for a beam of paramagnetic atoms such as silver or potassium [2]. Unlike the historical Stern-Gerlach experiment, however, the individual Zeeman components are not fully resolved due to the combined effects of finite molecular beam width, instrumental resolution limitations and spin-rotation interactions [17]. For the $V_n(C_6H_6)_{n+1}$ complexes, spatial broadening of the molecular beam is caused by the Zeeman splitting of the beam into $2S + 1$ equally-spaced *beamlets* [18]. In the case of $V(C_6H_6)_2$, the ground electronic state is $^2A_{1g}$ so that the number of the beamlets is taken to be $2S + 1 = 2$ [19]. In the beamlet model, broadened peak profile is expressed by a superposition of zero-field profiles. From the separation of beamlets as depicted in Figure 2a, the z-component of the magnetic moment, μ_z, for $V(C_6H_6)_2$ is found to be $0.7 \pm 0.1 \mu_B$ at source temperature of 154 K. The same procedure, applied to $V(C_6H_6)_2$ generated at 296 and 56 K yields magnetic moments of 0.7 ± 0.2 and $0.5 \pm 0.1 \mu_B$, respectively.

Figure 2b shows the PS-TOF profiles of $V_2(C_6H_6)_3$ recorded with the field gradient on and off. The plausible spin states for $V_2(C_6H_6)_3$ are singlet or triplet, corresponding to anti-parallel or parallel electron spin in d orbitals, respectively. The curve fitting analysis clearly reveals broadening of the beam, indicating that $V_2(C_6H_6)_3$ is not a singlet molecule. The observed broadening is well represented by the sum of three zero-field beamlets, equally spaced. From deflection of the outmost beamlet, the magnetic moment of $V_2(C_6H_6)_3$ was determined as $1.2^{+0.1}_{-0.2}\mu_B$ at 154 K. In a similar fashion, the magnetic moment of $V_2(C_6H_6)_3$ was determined as $1.2^{+0.2}_{-0.3}\mu_B$ at $T = 296$ K, and that of $V_3(C_6H_6)_4$ was determined as $1.5^{+0.2}_{-0.4}\mu_B$ and $1.9^{+0.5}_{-1.1}\mu_B$ at $T = 154$ and 296 K, respectively.

On the other hand, magnetic moments determined for $V_n(C_6H_6)_{n+1}$ clusters at $T = 56$ K were $0.5 \pm 0.1 \mu_B$, $1.0 \pm 0.4 \mu_B$, and $0.9^{+0.4}_{-0.5}\mu_B$, for $n = 2$, 3, and 4, respectively, considerably lower than the values obtained at higher temperatures. These reduced magnetic moments value and the suppression of size-dependence of the moments implies that the fragmentation involving loss of benzene occurs as a result of photoionization: $V_n(C_6H_6)_{n+1+p} \longrightarrow V_n(C_6H_6)_{n+1} + p\ C_6H_6$. As previously mentioned, benzene-rich clusters ($m > n + 1$ for $V_n(C_6H_6)_m$) were observed to be abundant at the colder source temperatures. This observation tells us that thermally unstable species (e.g. non-sandwich shaped clusters or complete $(n, n + 1)$ sandwich clusters containing additional, weakly adsorbed benzene) can survive in the cluster beam at colder conditions. Considering that the photofragmentation from non-sandwich clusters presumably results in the contamination in the PS-TOF signal measured for complete sandwich ions, the apparent magnetic moment could be smaller than the actual moments by as much as $0.5 \mu_B$ for $V_n(C_6H_6)_{n+1}$ clusters produced at colder temperatures. The similar problem, namely fragmentation of molecular clusters, has been discussed by Gedanken et al. in the deflection measurement of O_2, VCl_4 and OClO [20].

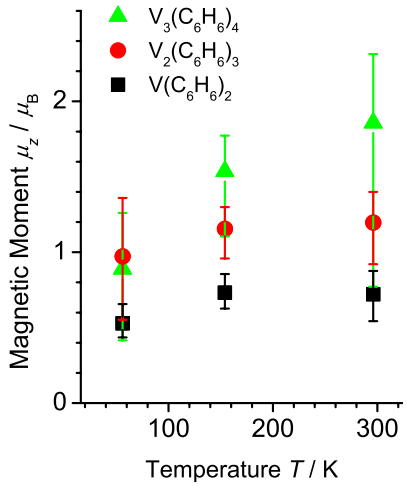

Fig. 3. Magnetic moments for $V_n(C_6H_6)_{n+1}$ clusters ($n = 1-3$) at $T = 56$, 154, and 296 K: solid square for (1, 2), solid circle for (2, 3), and solid triangle for (3, 4).

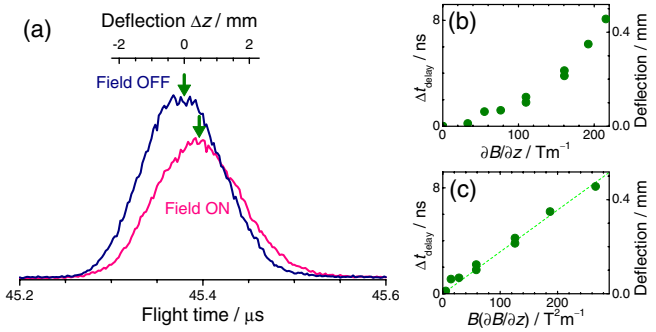

Fig. 4. Single-sided magnetic deflection of TOF peak profile of $Tb_3(C_8H_8)_4$ at $T = 146$ K with a field ON ($\partial B/\partial z = 216$ Tm^{-1}, $B = 1.23$ T) and OFF. Small plot (b) indicates the nonlinear relation between peak delay $\Delta t_{\rm delay}$ and magnetic field gradient $\partial B/\partial z$. Plot (c) is a rescaled version of peak delay $\Delta t_{\rm delay}$ vs. product of $B(\partial B/\partial z)$ for $Tb_3(C_8H_8)_4$.

Temperature dependence of the magnetic moments measured for $V_n(C_6H_6)_{n+1}$ clusters are summarized in Figure 3. Except for $T = 56$ K, each magnetic moment determined for $V_n(C_6H_6)_{n+1}$ ($n = 1-3$) remains unchanged (within experimental uncertainties) between $T = 154$ and 296 K. This result shows that the evaluation of magnetic moments for the $V_n(C_6H_6)_{n+1}$ clusters is free from the effects of photofragmentation of the non-sandwich clusters generated at or above $T = 154$ K. Furthermore, the increase of magnetic moments with size indicates that the spins of the non-bonding d electrons on the V metal centers align ferromagnetically, giving rise to monotonically-increasing magnetic moments. The mechanism of this ferromagnetic interaction among unpaired spins is qualitatively explained by a spin polarization on the intervened sandwich's LUMO. Recent theoretical (density functional theory) calculations put this qualitative picture on a quantitative footing, demonstrating that electron-spin multiplicities in the ground state are 2, 3 and 4 for $V_n(C_6H_6)_{n+1}$ ($n = 1-3$) [21]. It should be noted that observed magnetic moment corresponds to the outmost beamlet with $M_{S_{max}}$ smaller than the expected spin-only value of $n\mu_{\rm B}$. This discrepancy is attributed to the effects of spin-rotation interactions [22].

3.2 $Tb_n(C_8H_8)_{n+1}$ clusters

The photoionization mass spectra for terbium-cyclooctatetraene clusters also exhibit prominent peaks corresponding to $(n, n+1)$ stoichiometries that are characteristic of full multi-decker sandwich structures. Figure 4a shows the deflection profile of $Tb_3(C_8H_8)_4$ recorded with and without magnetic fields. As shown in the spectrum, the entire peak shifts to toward high field by the magnetic field gradient along with peak broadening. This behavior is qualitatively the same as has been observed for beams of ferromagnetic metal clusters (e.g., Ni_n, Co_n, Fe_n and Gd_n) [3–6] and is consistent with intramolecular spin relaxation occurring during the passage of the complexes through magnet. That intramolecular spin relaxation occurs for $Tb_n(C_8H_8)_{n+1}$ clusters (and not for $V_n(C_6H_6)_{n+1}$, which by contrast displays free-spin behavior, *vide supra*) can be attributed to the larger density of rovibronic states ρ predicted for these systems. In particular intramolecular spin relaxation can occur in isolated species only when the average spacing between rovibronic levels given by ρ^{-1} is less than spacing between Zeeman levels [22]. The electronic structure of $V_n(C_6H_6)_{n+1}$ clusters is comparatively simple owing to the non-bonding character of d_σ orbitals which accommodate unpaired spin. The density of states is sparse since there are no low-lying states which can be crossed in the magnetic field. In contrast, the density of states of $Tb_n(C_8H_8)_{n+1}$ clusters is dense due to existence of low-lying electronic states and mixing of these states in the presence of magnetic field. It is reasonable to expect that it is this large density of states that makes spin relaxation facile in $Tb_n(C_8H_8)_{n+1}$ clusters.

Figure 4c clearly shows a linear dependence of $B(\partial B/\partial z)$ against the spatial shift of the $Tb_3(C_8H_8)_4$ peak. This relationship is just the same as observed for ferromagnetic clusters of such as Fe_n [3–6]. Using equation (3), the intrinsic cluster moment for $Tb(C_8H_8)_2$ was determined to be 14 ± 1 $\mu_{\rm B}$ at $T = 146$ K. This value is larger than the magnetic moment of a free Tb^{3+} ion ($4f^8$; 9.7 $\mu_{\rm B}$).

Figure 5 shows the size dependence of magnetic moments for the $Tb_n(C_8H_8)_{n+1}$ sandwich clusters ($n = 1-5$). A monotonic increase of the magnetic moment with the size up to $n = 3$ is observed. For the $Tb_2(C_8H_8)_3$ sandwich cluster, a net magnetic moment can be roughly agreement with that estimated from $\sqrt{2}\mu_{\rm Tb(C_8H_8)_2}$ [23] implying that $Tb_n(C_8H_8)_{n+1}$ ($n = 1-2$) are paramagnetic. It has been reported by Ishii et al. [24] that magnetic exchange interactions occur between Ln-Ln ions in a Ln-phthalocyanine triple-decker complex for Ln = Tb and holmium (Ho). However, the temperature range in

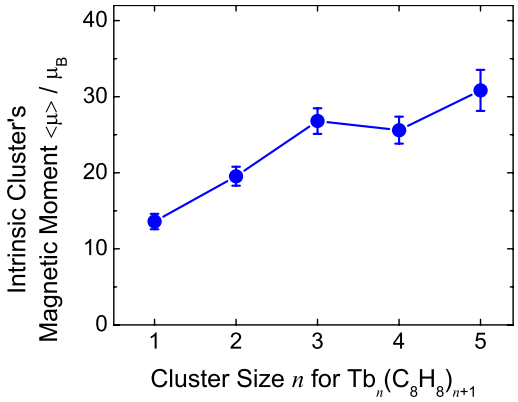

Fig. 5. Magnetic moments $\langle\mu\rangle$ for $Tb_n(C_8H_8)_{n+1}$ ($n = 1-5$) clusters at $T = 146$ K.

which they found antiferro-magnetic behavior is well below $T = 50$ K, and the deviation from the paramagnetic value is less than ∼10%. Since the temperature in this work was around $T = 150$ K, it seems reasonable to assume that the Tb^{3+} ions making up these complexes are not magnetically coupled, such that the magnetic moments for the $Tb_n(C_8H_8)_{n+1}$ sandwich ($n = 1-2$) do not exhibit significant deviation from simple paramagnetic behavior within experimental uncertainties.

As shown in Figure 5, the overall magnetic moment for $Tb_n(C_8H_8)_{n+1}$ drops slightly at $n = 4$, rather than increasing further. For clusters larger than $Tb_3(C_8H_8)_4$, the increase in magnetic moment with each subsequent Tb atom becomes smaller than observed for the smaller clusters. This non-additivity affect is ascribed to the particular oxidation states of Tb atoms making up the clusters. As reported previously [11], for longer sandwich clusters ($n > 2$), some of Tb atoms take on +2 oxidation states in addition to +3 states since the C_8H_8 ligand can accommodate two electrons: for $Tb_3(C_8H_8)_4$, the oxidation states of the constituents can be formally expressed as $(C_8H_8)^{2-}$ Tb^{3+} $(C_8H_8)^{2-}$ Tb^{2+} $(C_8H_8)^{2-}$ Tb^{3+} $(C_8H_8)^{2-}$. Similarly, for the case of $Tb_4(C_8H_8)_5$ cluster, two Tb^{2+} ions exist in the middle of the cluster, with the outermost Tb ions existing in +3 state. Since the magnetic moment for Tb^{2+} ($4f^9$; 9.47 μ_B) is almost the same as that of Tb^{3+} (9.7 μ_B), lower magnetic moments for $Tb_4(C_8H_8)_5$ cluster implies that interaction between the two central Tb^{2+} ions is antiferromagnetically coupled, with the Tb^{3+} ions remaining uncoupled (paramagnetic). The increase of magnetic moment from $n = 4$ to $n = 5$ can be explained by the excess Tb^{2+} ion which cannot be coupled. Therefore continued zigzag oscillation of magnetic moments is expected to $Ln_n(C_8H_8)_{n+1}$ clusters ($n \geq 3$).

In fact, similar even-odd alternation of the magnetic moments has been observed also for $Ho_n(C_8H_8)_{n+1}$ ($n = 3-7$) at $T = 54$ K. The same trend can be also found in other measurements for $Ho_n(C_8H_8)_{n+1}$ ($n = 3-5$) at $T = 152$ K, $Gd_n(C_8H_8)_{n+1}$ ($n = 3-5$) at $T = 60$ K and $Tb_n(C_8H_8)_{n+1}$ ($n = 3-5$) at $T = 61$ K [25]. Although mechanism for this even-odd alternation phenomenon remains to be examined in detail theoretically, we surmise that it is due to antiferromagnetic spin-spin interaction between adjacent Ln^{2+} ions within the Ln-C_8H_8 sandwich cluster.

In summary, the magnetic deflections of multi-decker vanadium-benzene and terbium-cyclooctatetraene organometallic clusters have been measured by a Stern-Gerlach molecular beam deflection experiment. The beams of $V_n(C_6H_6)_{n+1}$ clusters were symmetrically broadened by a magnetic gradient, and monotonic increase of the magnetic moments of $V_n(C_6H_6)_{n+1}$ clusters up to $n = 4$ was found. On the other hand, $Tb_n(C_8H_8)_{n+1}$ sandwich species displayed one-side deflection which indicates the occurrence of fast intramolecular spin relaxation. The evolution of the magnetic moment with the size can be explained solely by the number of Tb^{3+} ions, suggesting antiferromagnetic interaction of two adjacent Tb^{2+} ions toward the center of the complex. Pinning by soft-landing of size-selected clusters onto nano-scale designed surfaces is an emerging approach [26] that is expected to open exciting new possibilities for exploiting these species as nano-sized magnetic building blocks in applications such as recording media or spintronic devices.

This work was performed under the auspices of the Office of Science, Division of Chemical Science, US-DOE under contract number W-31-109-ENG-38. This work is partly supported by the 21st Century COE program "KEIO Life Conjugate Chemistry" (KEIO-LCC) from the Ministry of Education, Culture, Sports, Science, and Technology, Japan.

References

1. A. Nakajima, K. Kaya, J. Phys. Chem. A **104**, 176 (2000)
2. W.D. Knight, R. Monot, E.R. Dietz, A.R. George, Phys. Rev. Lett. **40**, 1324 (1978)
3. D.M. Cox, D.J. Trevor, R.L. Whetten, E.A. Rohlfing, A. Kaldor, Phys. Rev. B **32**, 7290 (1985)
4. W.A. de Heer, P. Milani, A. Châtelain, Phys. Rev. Lett. **65**, 488 (1990); W.A. de Heer, P. Milani, A. Châtelain, Z. Phys. D **19**, 241 (1991)
5. D.C. Douglass, A.J. Cox, J.P. Bucher, L.A. Bloomfield, Phys. Rev. B **47**, 12874 (1993)
6. I.M.L. Billas, A. Châtelain, W.A. de Heer, Science **265**, 1682 (1994); I.M.L. Billas, A. Châtelain, W.A. de Heer, J. Mag. Mag. Mater. **168**, 64 (1997); D. Gerion, A. Hirt, A. Châtelain, Phys. Rev. Lett. **83**, 532 (1999)
7. A. Amirav, G. Navon, Chem. Phys. **82**, 253 (1983)
8. K. Hoshino, T. Kurikawa, H. Takeda, A. Nakajima, K. Kaya, J. Phys. Chem. **99**, 3053 (1995); K. Miyajima, K. Muraoka, M. Hashimoto, T. Yasuike, S. Yabushita, A. Nakajima, K. Kaya, J. Phys. Chem. A **106**, 10777 (2002)
9. T. Yasuike, S. Yabushita, J. Phys. Chem. A **103**, 4533 (1999)
10. W. Liu, M. Dolg, P. Fulde, J. Chem. Phys. **107**, 3584 (1997)
11. K. Miyajima, T. Kurikawa, M. Hashimoto, A. Nakajima, K. Kaya, Chem. Phys. Lett. **306**, 256 (1999)
12. T. Kurikawa, Y. Negishi, F. Hayakawa, S. Nagao, K. Miyajima, A. Nakajima, K. Kaya, J. Am. Chem. Soc. **120**, 11766 (1998)

13. F. Mares, K. Hodgson, A. Streitwieser Jr, J. Organomet. Chem. **24**, C68 (1970); K.O. Hodgson, F. Mares, D.F. Starks, A. Streitwieser Jr, J. Am. Chem. Soc. **95**, 8650 (1973)
14. M.B. Knickelbein, J. Chem. Phys. **116**, 9703 (2002)
15. W.A. de Heer, P. Milani, Rev. Sci. Instrum. **62**, 670 (1991)
16. S.N. Khanna, S. Linderoth, Phys. Rev. Lett. **67**, 742 (1991)
17. K. Miyajima, A. Nakajima, S. Yabushita, M.B. Knickelbein, K. Kaya, J. Am. Chem. Soc. **126**, 13202 (2004)
18. N.F. Ramsey, *Molecular Beams* (Oxford University Press, Oxford, 1956)
19. E.O. von Fisher, G. Joos, W. Meer, Z. Naturf. **13b**, 456 (1958); F.G.N. Cloke, A.N. Dix, J.C. Green, R.N. Perutz, E.A. Seddon, Organometallics **2**, 1150 (1983); A. McCamley, R.N. Perutz, J. Phys. Chem. **95**, 2738 (1991); M.P. Andrews, S.M. Mattar, G.A. Ozin, J. Phys. Chem. **90**, 744 (1986); M.P. Andrews, S.M. Mattar, G.A. Ozin, J. Phys. Chem. **90**, 1037 (1986); S.E. Anderson Jr, R.S. Drago, J. Am. Chem. Soc. **92**, 4244 (1970)
20. A. Gedanken, N.A. Kuebler, R.B. Robin, D.R. Herrick, J. Am. Chem. Soc. **111**, 5568 (1989); A. Gedanken, V. Kelner, E. Sominska, Chem. Phys. Lett. **221**, 274 (1994)
21. A.K. Kandalam, B.K. Rao, P. Jena, R. Pandey, J. Chem. Phys. **120**, 10414 (2004); J. Wang, P.H. Acioli, J. Jellinek, J. Am. Chem. Soc. (in press, 2005)
22. M.B. Knickelbein, J. Chem. Phys. **121**, 5281 (2004); K. Miyajima, S. Yabushita, M.B. Knickelbein, A. Nakajima (in preparation)
23. M. Schultz, J.M. Boncella, D.J. Berg, T.D. Tilley, R.A. Andersen, Organometallics **21**, 460 (2002)
24. N. Ishikawa, T. Iino, Y. Kaizu, J. Am. Chem. Soc. **124**, 11440 (2002)
25. K. Miyajima, S. Yabushita, M.B. Knickelbein, A. Nakajima (in preparation)
26. K. Judai, K. Sera, S. Amatsutsumi, K. Yagi, T. Yasuike, S. Yabushita, A. Nakajima, K. Kaya, Chem. Phys. Lett. **334**, 277 (2001)